Photoinduced Stiffening in ZnO Nanobelts

M. H. Zhao,[1,*] Zhi-Zhen Ye,[2] and S. X. Mao[1,2,†,‡]

[1]*Department of Mechanical Engineering & Materials Science, University of Pittsburgh, Pittsburgh, Pennsylvania 15261, USA*
[2]*Department of Materials Science & Engineering, Zhejiang University, Zhejiang, 310027, P.R. China*

(Received 4 September 2008; published 29 January 2009)

We report the observation of remarkable photoinduced stiffening in a single ZnO nanobelt using nanoindentation and atomic force microscopy. The apparent elastic modulus of a ZnO nanobelt under illumination with a photon energy greater than the band gap becomes much larger than that under darkness. The physical mechanism for the observed phenomena is analyzed in terms of the surface effect and the electronic strain induced by the photogeneration of free carriers in a ZnO nanobelt.

DOI: 10.1103/PhysRevLett.102.045502 PACS numbers: 62.20.−x

A ZnO nanobelt, an 1D nanostructure with a rectangular cross section [1], has unique mechanical [2] and piezoelectric properties [3], which are very different from its bulk. Although the photoelastic effect, in which the optical properties (refractive index) of ZnO can be modified by elastic stress or strain, has been reported [4–6], the inverse effect, the influence of light on the elastic properties of ZnO, has never been reported. Here we report the first observed photoinduced reversible stiffening in a single ZnO nanobelt by nanoindentations and atomic force microscopy (AFM), while such effect is not observed in ZnO bulk. The physical mechanism for the observed phenomena is analyzed in terms of the surface effect and the electronic strain induced by the photogeneration of free carriers in ZnO.

ZnO nanobelts were prepared and dispersed onto the Si substrate as described before [1–3]. Nanoindentations on a ZnO nanobelt and (0001) bulk ($5 \times 5 \times 0.5$ mm, supplied by M.T.I. Corp.) were done by the Hysitron Triboscope nanoindenter and the Veeco Nanoscope IIIa Multimode AFM. In case of the nanoindentions by the Hysitron Triboscope, the sample was illuminated by a mercury lamp and a fiber illuminator at an angle of incidence $\alpha = 20°$. A cube corner diamond indenter was used to image a ZnO nanobelt and then *in situ* indent the nanobelt with the same tip. The loading and unloading rate was kept constant at 10 μN/s. After nanoindentations, the impression was imaged with the same tip, which verified that the test was performed in the anticipated location as shown in Fig. 1. The thickness of the investigated ZnO nanobelt estimated from Fig. 1 was ~250 nm, which restrained the nanoindentation depth below 80 nm, as it was generally accepted that the depth of indentation should not exceed 30% of the wire diameter or film thickness [7]. An elastic modulus of a ZnO nanobelt can be derived from unloading part of a load-displacement curve using the Oliver and Pharr method [8].

Comparison of nanoindentations on the ZnO nanobelt with and without illumination reveals a marked difference in the load-displacement curve (Fig. 2). Although the plastic deformation after unloading is similar in the two cases, the total deformation (elastic plus plastic deformation) with illumination during loading is much smaller than that without illumination, which implies that the elastic deformation in darkness is much larger than that in light. As the load in two cases is similar, different elastic deformation means the change of elastic property, which is defined as apparent elastic modulus thereafter. The reason for this definition is related to the mechanism of the observed effect, which will be discussed later. This is consistent with the results derived from unloading part of the load-displacement curve (Fig. 3) using the Oliver-Pharr method. Figure 3 provides a comparison of illumination induced stiffening between a ZnO nanobelt and (0001) bulk. While there is little change of the apparent elastic modulus in ZnO bulk after illumination, the increase of the apparent elastic modulus in the ZnO nanobelt by illumination is at least 200% in the indentation depth from 10 to

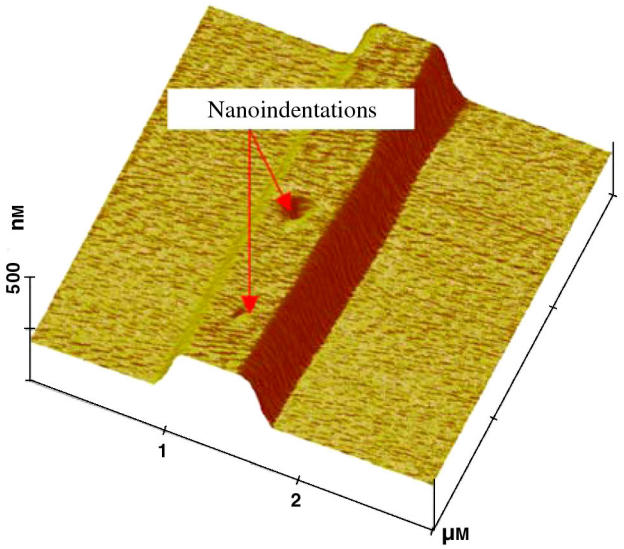

FIG. 1 (color online). Images of nanoindentations on the ZnO nanobelt by the Hysitron Triboscope.

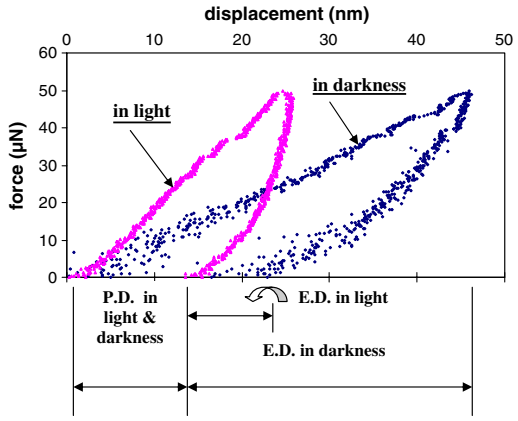

FIG. 2 (color online). Comparison of load-displacement curves of the ZnO nanobelt by nanoindentations with and without illumination (P.D. stands for plastic deformation, E.D. stands for elastic deformation).

80 nm. Furthermore, the effect is reversible. The stiffening effect will disappear when the light is turned off.

On the other hand, the elastic modulus estimated from the unloading stiffness [8] is impossible to exclude the effect of inelastic processes, as unloading is not a purely elastic process [9]. Furthermore, there is an increase in the effect of inelastic processes on the unloading curve with increasing maximum load, which ranges from 20 to 200 μN currently. Further decreasing the maximum load on a ZnO sample by Triboscope will result in the unacceptable scattering of the data. That is why an alternative indentation method was used to study this phenomenon.

The other nanoindentation method was performed with the Nanoscope IIIa Multimode AFM using stainless steel cantilever with a diamond tip. In this case, an inline filter box (FHS-UV from Ocean Optics Inc.) was applied between the light source and the fiber illuminator. Two kinds of filters were used during illumination. One was a 360 nm band-pass filter, which provided illumination with photon energy higher than the band gap of ZnO (3.34 eV or ~380 nm). The other was a 550 nm high pass filter, which gave illumination with photon energy lower than the band gap of ZnO. The spring constant of the cantilever was calibrated by Veeco Instruments to be 286.2 N/m. A diamond tip with tetrahedric geometry (a three sided pyramid with an apex angle of 60 degrees and a nominal tip radius of 25 nm) was mounted to the end of the cantilever in a way that the vertical axis of the pyramid was approximately normal to the sample surface. Before nanoindentation, the nanobelt was located by the diamond tip under the tapping mode. Then the tip was positioned at the center of the nanobelt. Ultra low load (below 1 μN) was applied during nanoindentation to ensure purely elastic deformation, as well as the contact between the tip and the sample was mainly spherical and could be described as Eq. (1) using the Hertzian model:

$$F = \tfrac{4}{3}E^* R^{1/2} h^{3/2}, \tag{1}$$

where F is the indentation load, E^* is the apparent elastic modulus of the tip-sample system. When the tip elastic modulus is much larger than that of sample E, $E \approx E^*$. R is the tip radius and h is the penetration depth in the sample. F and h can be experimentally derived from Eqs. (2) and (3).

$$F = k_c d_c = k_c \Delta U_c \tag{2}$$

$$h = z - d_c = z - \Delta U_c, \tag{3}$$

where k_c is the spring constant of the cantilever and d_c is the cantilever deflection, z represents the piezo-scanner movement along the vertical direction and U_c is the cantilever deflection signal.

As z and U_c are directly available from the experiment (Fig. 3) and $k_c = 286.2$ N/m, the key step to determine the F-h curve using Eqs. (2) and (3) is to find out the cantilever sensitivity Δ. This sensitivity is the ratio of the Z motion of the piezo measured in nm, to the cantilever deflection measured in volts. Its units are nm/volt and are determined from the slope of the force-plot curve by indenting on a hard surface such as sapphire with a Young's modulus of 470 GPa [9]. Under such circumstances, the penetration depth in the sample is negligible, which means $h \approx 0$ and $z \approx d_c$. Hence $\Delta \approx z/U_c$.

Once the F-h curve is derived, we can find out E^* and R by parameter fitting using Eq. (1). However, there are two parameters involved in the fitting and R should be a fixed constant as long as the tip is not blunted during indentation. So we find out R by nanoindenting on the fused quartz in the elastic region, of which the reduced Young's modulus is well known to be 69.6 GPa. The average results of fitting to ten F-h curves give $R = 18 \pm 2$ nm, which is close to manufacture's specification. Once R is known, one parameter fitting to Eq. (1) gives E^*. Figure 4 is a comparison of a typical force-penetration relation of a ZnO nanobelt under 360 nm UV illumination, 550 nm high pass illumination, and in darkness. The marks are the average of 5 experimental measurements and the lines are fitted by the

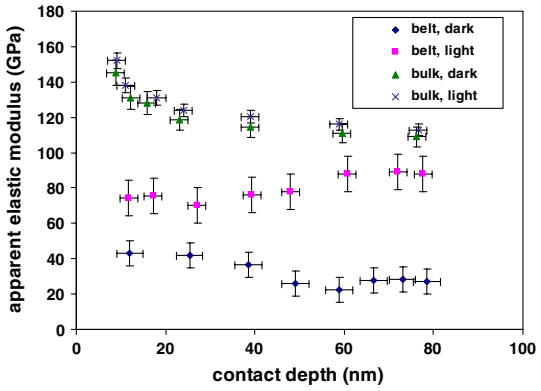

FIG. 3 (color online). Comparison of the apparent elastic modulus of the ZnO nanobelt and (0001) bulk by nanoindentations in darkness and in light.

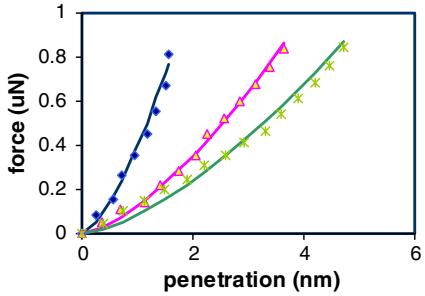

FIG. 4 (color online). Comparison of a typical force-penetration curve of the ZnO nanobelt by a cantilever-typed diamond indenter under different illumination. Symbols of diamonds, triangles, and crosses are experimental data under 360 nm UV, 550 nm high pass illumination, and no illumination, respectively. The lines are fitted by the Hertzian model using Eq. (1).

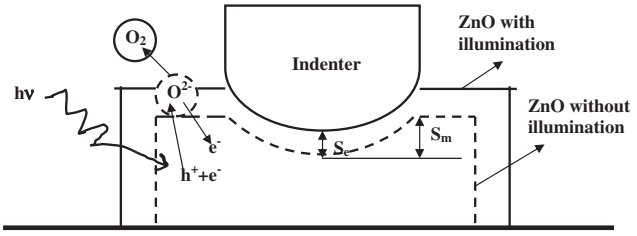

FIG. 5. Schematic of the surface response of ZnO by nanoindentations with and without illumination. Without illumination, the surface response of ZnO (dotted line) by nanoindentation is S_m and there are oxygen ions adsorbed on the surface. With illumination, the surface expanded (solid line) and the corresponding deformation due to the electronic strain is S_e, which gives the net surface response $S_m - S_e$. In the meantime, holes produced by the illumination discharge the negatively charged oxygen ions on the ZnO surface, which results in extra free electrons in the ZnO.

Hertzian model. First, the one-parameter fitting by the Hertzian model matches perfectly to the experiment, which indicates that the contact between the indenter and the ZnO nanobelt can be described as Hertzian elastic. Second, the apparent elastic modulus of the ZnO nanobelt in darkness and 550 nm high pass illumination is 15 ± 3 GPa and 22 ± 4 GPa, respectively, while it is 70 ± 14 GPa under 360 nm UV illumination and almost independent of the intensity of the illumination ($\sim$1–100 mW/cm^2). Third, we find the photoinduced stiffening in the ZnO nanobelt is reversible. These results provide us with the following information. (i) Elasticity of the ZnO nanobelt is sensitive to the UV illumination (above the band gap of ZnO 380 nm) and not sensitive to the illumination with photon energy lower than the band gap and light intensity. (ii) The apparent elastic modulus of the ZnO nanobelt derived from the loading part of the force-penetration depth curve below 5nm using Hertzian model is comparable to that determined by the unloading part of the nanoindentation curve below 80 nm using the Oliver and Pharr method. Both results are in agreement with the derived values from the TEM resonance method, which ranges from 40–60 GPa [10]. In contrast, there is little difference in the apparent elastic modulus of the ZnO bulk with and without illumination, which varies between 100 to 120 GPa (Fig. 3).

The physical mechanism for the observed stiffening phenomena can be related to the electronic strain induced by the photogeneration of free charge carriers in ZnO. It is well known that the injection of free carriers results in the local mechanical straining of a semiconductor [11–13]. By illumination with photons of energies above the ZnO band gap, electron-hole pairs are generated. The electronic strain in the illuminated diamond-type semiconductor is in the form of [11–13],

$$S_e = \frac{1}{3}\frac{d\varepsilon_g}{dP}\Delta n, \tag{4}$$

where $d\varepsilon_g/dP$ is the pressure dependence of the band gap energy; Δn is the density of the photogenerated excess charge carriers expressed in cm^{-3}. As the expression of the electronic strain for ZnO was not available, we treat the photoinduced electronic strain similar to the case of silicon. As shown in Fig. 5, the surface response of ZnO (segmented line) by nanoindentation is S_m without illumination. According to Eq. (4), the electronic strain in ZnO under illumination will be positive since the pressure dependence of the band gap energy is positive for ZnO ($\sim$24.5 meV/GPa $= 3.92 \times 10^{-24}$ cm^3 for ZnO [14]). This results in the expansion of the ZnO with illumination. The surface expands (Fig. 5, solid line) and the corresponding deformation due to the electronic strain is S_e. Hence, the electronic strain as a result of photo-generated free charge carriers resists the mechanical strain caused by the indent. The net surface response S_t under illuminated indentation is given by Eq. (5),

$$S_t = S_m - S_e = \frac{\sigma}{E} - \frac{1}{3}\frac{d\varepsilon_g}{dP}\Delta n = \left(\frac{1}{E} - \frac{1}{3}\frac{d\varepsilon_g}{dP}\frac{\Delta n}{\sigma}\right)\sigma, \tag{5}$$

where S_m is the mechanical strain caused by the indentation, σ is the mechanical stress, and E is the elastic modulus. In addition, we define the apparent elastic modulus measured by the illuminated nanoindentation as

$$\frac{1}{E_{\text{app}}} \equiv \frac{1}{E} - \frac{1}{3}\frac{d\varepsilon_g}{dP}\frac{\Delta n}{\sigma} \Rightarrow \frac{E}{E_{\text{app}}} = 1 - \frac{1}{3}\frac{d\varepsilon_g}{dP}\frac{E\Delta n}{\sigma}. \tag{6}$$

To determine the effect of the illumination on the elastic modulus, it is critical to estimate the magnitude of the second term in Eq. (6). For ZnO, the mean compressive stress caused by nanoindentation can be estimated to be $\sigma = F/\pi R\delta$ [15], where F is the load of the nanoindentation, R is the radius of the indenter, and δ is the penetration depth. If taking $F = 0.5$ μN, $R = 18$ nm, and $\delta = 2$ nm, we estimate $\sigma \approx 5$ GPa. From Eq. (6), the apparent elastic modulus under illumination is greater than that under dark-

ness if the photoinduced density of charge carriers Δn is positive.

In the dark, oxygen molecules adsorb on the ZnO surface as negatively charged ions by capturing free electrons from the n-type ZnO and create an electron depletion layer near surface [16]. Upon exposure to photons with energy greater than the band gap of ZnO, electron-hole pairs were generated in ZnO. Photo-generated holes then migrate to the surface and discharge the negatively charged oxygen ions on the ZnO surface (Fig. 5). Hence, the photo-generated electrons can increase the density of free charge carriers Δn near the surface as ZnO is normally an n-type semiconductor [17]. To better understand the different case in the ZnO belt and bulk, we will distinguish the increase of the free charge density by the following two contributions:

$$\Delta n = \Delta n_p + \Delta n_d, \tag{7}$$

where Δn_p is the contribution from the photoinduced electron-hole pairs ($h\gamma \rightarrow h^+ + e^-$), and Δn_d is the contribution from the desorption of the oxygen gas on the surface ($O_2^- + h^+ \rightarrow O_2$ or $O^{2-} + h^+ \rightarrow O_2 + e^-$). It is important to note that the penetration depth for photons with energies greater than the band gap of ZnO is only approximately 100 nm [18]. Since the thickness of the ZnO nanobelt is comparable to the penetration depth of UV light, the whole cross section of the nanobelt may be photo activated and become an electron rich layer, while only the surface of the ZnO bulk is photo activated. Because of the diffusion of free carriers, we can conclude $\Delta n_{p,\mathrm{belt}} \gg \Delta n_{p,\mathrm{bulk}}$ during illumination. Furthermore, as the nanobelt has a much higher surface to volume ratio than the bulk, there will be more chance for the photo-generated holes to be discharged on the surface of the nanobelt than those of the bulk. Hence, $\Delta n_{d,\mathrm{belt}}$ is also larger than $\Delta n_{d,\mathrm{bulk}}$ during illumination. In fact, the high density of electron carriers in the ZnO nanobelt was manifested by several *orders* of increase of the current upon UV illumination (supplemental Fig. S2 [19], and Refs. [16–18,20]), compared to only several *times* of increase in the ZnO bulk [18]. Therefore, we can predict that the photoinduced electronic strain would be much greater in the ZnO nanobelt than that in the ZnO bulk due to the surface effect, which is the reason why photoinduced stiffening was only observed on the ZnO nanobelt surface. When light was turned off, the recombination of electron-hole and reabsorbed oxygen on the ZnO surface reduced the density of free charge carriers, which resulted in less contribution from electronic strain. Hence the photoinduced stiffening effect in a ZnO nanobelt is reversible.

In conclusion, strong photoinduced stiffening effect was observed for the first time in a single ZnO nanobelt by nanoindentations. The observed remarkable photoinduced elastic effect in 1D semiconducting nanostructures has theoretical and practical significance. Theoretically, electronic strain may play an important role in the mechanical deformation of 1D semiconducting nanostructures under illumination with photon energy greater than the band gap of the semiconductor, demonstrating the significance of mechanical, optical, and electronic coupling in 1D nanostructures. Practically, our experimental results indicate that elastic properties of 1D ZnO nanostructures may be tuned by the optical illumination, which sheds light on realizing nanoscale optical tunable surface acoustic wave devices based on 1D ZnO nanostructures.

This work was supported in part by the National Science Foundation (CMS-0140317). The authors thank Professor Z. L. Wang of George Institute of Technology for providing ZnO nanobelt samples and helpful discussions.

*Current affiliation: National Research Council NIST/NIH joint program
†Corresponding author.
‡smao@engr.pitt.edu

[1] Z. W. Pan, Z. R. Dai, and Z. L. Wang, Science **291**, 1947 (2001).
[2] S. X. Mao, M. H. Zhao, and Z. L. Wang, Appl. Phys. Lett. **83**, 993 (2003).
[3] M. H. Zhao, Z. L. Wang, and S. X. Mao, Nano Lett. **4**, 587 (2004).
[4] R. Berkowicz and T. Skettrup, Phys. Rev. B **11**, 2316 (1975).
[5] H. Sasaki, K. Tsubouchi, and N. Mikoshiba, J. Appl. Phys. **47**, 2046 (1976).
[6] T. Azuhata *et al.*, J. Appl. Phys. **94**, 968 (2003).
[7] B. Bhushan and X. D. Li, Int. Mater. Rev. **48**, 125 (2003).
[8] W. C. Oliver and G. M. Pharr, J. Mater. Res. **7**, 1564 (1992).
[9] Y. M. Soifer and A. Verdyan, Phys. Solid State **45**, 1701 (2003).
[10] X. D. Bai, P. X. Gao, and Z. L. Wang, Appl. Phys. Lett. **82**, 4806 (2003).
[11] R. G. Stearns and G. S. Kino, Appl. Phys. Lett. **47**, 1048 (1985).
[12] P. G. Datskos, S. Rajic, and I. Datskou, Appl. Phys. Lett. **73**, 2319 (1998).
[13] D. M. Todorovic, P. M. Nikolic, and A. I. Bojicic, J. Appl. Phys. **85**, 7716 (1999).
[14] A. Segura *et al.*, Appl. Phys. Lett. **83**, 278 (2003).
[15] J. Caro, F. Fraxedas, P. Gorostiza, and F. J. Sanz, J. Vac. Sci. Technol. A **19**, 1825 (2001).
[16] H. kind *et al.*, Adv. Mater. **14**, 158 (2002).
[17] Y. W. Heo *et al.*, Appl. Phys. Lett. **85**, 2002 (2004).
[18] L. Carlsson and C. Svensson, J. Appl. Phys. **41**, 1652 (1970).
[19] See EPAPS Document No. E-PRLTAO-102-051906 for supplemental material. For more information on EPAPS, see http://www.aip.org/pubservs/epaps.html.
[20] K. Keem *et al.*, Appl. Phys. Lett. **84**, 4376 (2004).